



HAL
open science

Spatial Sampling and Integrity in Lane Grid Maps

Corentin Sanchez, Philippe Xu, Alexandre Armand, Philippe Bonnifait

► **To cite this version:**

Corentin Sanchez, Philippe Xu, Alexandre Armand, Philippe Bonnifait. Spatial Sampling and Integrity in Lane Grid Maps. 32nd IEEE Intelligent Vehicles Symposium (IV 2021), Jul 2021, Nagoya, Japan. pp.190-196, 10.1109/IVWorkshops54471.2021.9669257 . hal-03327985

HAL Id: hal-03327985

<https://hal.science/hal-03327985>

Submitted on 27 Aug 2021

HAL is a multi-disciplinary open access archive for the deposit and dissemination of scientific research documents, whether they are published or not. The documents may come from teaching and research institutions in France or abroad, or from public or private research centers.

L'archive ouverte pluridisciplinaire **HAL**, est destinée au dépôt et à la diffusion de documents scientifiques de niveau recherche, publiés ou non, émanant des établissements d'enseignement et de recherche français ou étrangers, des laboratoires publics ou privés.

Spatial Sampling and Integrity in Lane Grid Maps

Corentin Sanchez¹, Philippe Xu¹, Alexandre Armand² and Philippe Bonnifait¹

Abstract—Autonomous vehicles have to take cautious decisions when driving in complex urban scenarios. Situation understanding is a key point towards safe navigation. High Definition maps supply different types of prior information such as road network topology, geometric description of the road, and semantic information including traffic laws. Conjointly with the perception system, they provide representations of the static environment and allow to model interactions. For safety issues, it is crucial to get a reliable understanding of the vehicle situation to avoid inappropriate decisions. Confidence on the information supplied to decision-making must be therefore provided. This paper proposes a spatial occupancy information representation at lane level with Lane Grid Maps (LGM). Based on areas of interest for the ego vehicle and sampled in the along-track direction, perception data is augmented to provide non-misleading information to the decision-making at a tactical level. An advantage of this representation is its ability to manage information integrity thanks to a good spatial sampling choice. The proposed approach takes into account the uncertainty of the ego vehicle localization, which has an impact on the estimated spatial occupancy of the perceived objects. This paper provides a method to set the proper sampling step in order to avoid oversampling and subsampling of the LGM for a given integrity risk level. The approach is evaluated with real data obtained thanks to several experimental vehicles.

I. INTRODUCTION

A key capability of autonomous vehicles (AV) is to take the best decision in every situation it encounters. In order to achieve this task, the decision-making (DM) module in the architecture of the AV needs to have a good understanding of the surrounding of the ego vehicle. Operating in urban areas remains challenging for autonomous driving systems. Thus, the information provided to the DM module must not be misleading so that proper decisions can be made. For example, characterizing a driving space as free when it is actually occupied may lead to a hazardous decision. Our work stands between the DM module and its raw input data provided by the perception and localization modules. Indeed, as data is provided by sensors, information is extracted by the perception module but still needs to be understood in order to take the best decision. This paper aims at providing an augmented information representation that takes into account information brought by the perception as well as information stored in a multi-layer map. The purpose is to get a better understanding of the situation that is supplied to the DM module. Such a representation can be generated within our

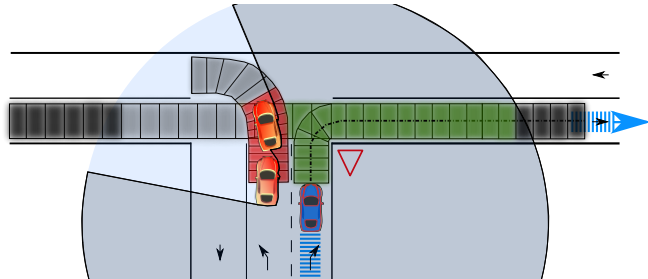


Fig. 1: Lane Grid Map representation. Areas Of Interest of the ego vehicle in blue are sampled. Cells are characterized by different states: Free (green), Occupied (red), Hidden (gray), out field of view (black).

so-called world model module which purpose is to enhance situation understanding.

In several architectures, the DM system can be seen as a tripartite module [1]. It works under three abstraction levels, which correspond to different levels of decision. At the lowest level (operational level), there is the local planning system that handles local and short term trajectories [2]. At the intermediate level (tactical level), the maneuver planner takes decisions on tasks that have to be achieved at a lane level [3]. Finally, at the most abstracted layer (strategic level) the global planner plans long-term decisions such as the itinerary to follow to complete the mission. In order to plan trajectories at a low level, two types of approaches can be highlighted. The first one is to use objects lists and to navigate through the obstacles [4], [5]. In this case there is no explicit information on the absence of objects, and occlusions have to be handled [6], [7]. In addition, there is a need to get spatial information. Another approach is to use occupancy grids [8] or free space polygons [9] to plan the trajectories. However there is a limitation if the vehicle operates in a complex environments with multiple interactions. The use of maps is necessary to add context, and thus to facilitate situation understanding [10]. Using maps implies to have reliable localization of the ego vehicle, in order to project perception information onto the map. Therefore, the integrity of the localization needs to be properly considered [11]. At the intermediate level, the maneuver planner enables to take into account this context as it is shown in the “environment model” mentioned in [3].

In this work, we propose a lane level information representation at tactical level, that handles occlusions and enables to improve confidence on information. In addition, it reduces the risk of providing misleading information to the DM module. An HD map is used to infer the lanes of interest as presented in [12], and to infer their occupancy through an along-track sampling as illustrated in figure 1. The sampling

This work has been carried out within **SIVALab**, a shared laboratory between **Renault** and **Heudiasyc** (UTC/CNRS), and financed by the **CNRS**.

¹Université de technologie de Compiègne, CNRS, Heudiasyc, CS60319 -60203 Compiègne Cedex, France

²Renault S.A.S, Guyancourt, France

step will be the key stone to handle the integrity of the generated information. We propose an evaluation method which combines both spatial information and distance metrics. These are our main contributions. Related work is discussed in Section II. Section III introduces the Lane Grid Map and its principles. The evaluation method is explained in section IV and is followed by the integrity bought by this representation in section IV-B. Finally, results are presented in section V.

II. RELATED WORK

In our world model representation, as previously introduced in [12], in a similar correspondence with the DM module, the notion of abstraction levels is early introduced with [13] and reused for decision-making [1]. There are three levels. From the lowest to the highest we have respectively the operational level, the tactical level and the strategic level. Each level operates in its own representation area from local with the lowest level to global with the highest.

Information representation used as inputs to these levels of the decision-making is therefore a key point. First, we need to dissociate discrete representation like with objects with spatial representations. In [5] or in [14], objects and features are used to represent the vehicle surroundings. Maps also contain at each level of abstraction different information: topological, semantic and geometric information as in [15]. However, unlike objects, spatial information enables to characterize surfaces and to give information on missing information. Among this kind of representation we could cite grids: probabilistic grids [16], evidential grids [17], interval maps [18] or even more than 2D representations as with [19]. There is also a more compact representation with polygon approaches as with the parametric free space presented in [9]. All these representations are built thanks to the perception system.

For decision-making evaluation, the metric often used is distances based on the situation encountered by the vehicle. It can be expressed as Time-To-Collision (TTC) or Enhanced-Time-To-Collision (ETTC) [20] or even Time-To-Entrance (TTE) [21]. Even more complex evaluation models are used for safety evaluation such as the Responsibility-Sensitive Safety (RSS) model [22]. We therefore want to combine the advantages of both representations, i.e using distances and spatial occupancy, to supply non-misleading information at the maneuver level.

In order to manage confidence of information and risk to provide misleading information, the notion of integrity can be cited. This criterion has been developed and formalized in the aviation field. It has been explored for urban environments as presented in [23]. This notion of integrity has also been applied for localization systems for instance [11]. Given an integrity risk, the system should not underestimate the uncertainty we can have on input values.

In this paper we want to enhance spatial information by using a low level spatial information representation but also give a distance metric and confidence over the information supplied to the decision-making module. We reuse the notion

of integrity to guarantee a functional operating domain for the AV through the sampling method of the Lane Grid Map. We show that oversampling can lead to integrity loss.

III. LANE GRID MAP

In a world model system, the three levels of abstraction provide a hierarchy of levels with several types of information representation. Each level has a specific type of task to achieve. As this paper focuses on the spatial representation layer, it aims at describing and evaluating a tactical level representation. This representation shown in figure 1 is called a Lane Grid Map (LGM). This section aims at describing our approach on an intermediate level representation that contains information with a high integrity level for handling non-misleading situation representation in order to enhance the DM process. Indeed, in order to be able to get on the road, an absence of vehicle is not enough. It is also necessary that the space is free and that this information has a high confidence value. We show that this representation enables to handle and guarantee a confidence level of integrity of the information taking into account localization uncertainty thanks to a sampling step parameter.

A. Principles

In order to build the LGM, we need to define the areas that are of interest for the AV. At the strategic level we are able to construct the Areas Of Interest (*AOI*) tree of the AV under the Interaction Graph named representation (right part of figure 2). Each node of the Interaction Graph is a portion of the *AOI* that describes in two ways the most important part of the vehicle surroundings. These *AOI* are built by the primary order lanes and secondary order lanes. Primary lanes are road lanes that are in direct interaction with the ego vehicle path. Secondary lanes correspond to lanes that are in direct interaction with the primary lanes but not in direct interaction with the ego vehicle path. These primary and secondary order represent road lanes extracted from the topological layer of an HD map where the ego vehicle must focus its attention in order to take best decisions and should not provide misleading information. These concepts are detailed in [12].

At the tactical level, we use the Interaction Graph nodes and the geometric information of the HD Map to build a lane level spatial representation (center part of figure 2). Thus, the LGM depends on the context in which the AV drives and is a discrete representation of the *AOI* made of cells.

B. Spatial sampling process

The cells are contiguous and have a sampling step parameter. In our case, at the tactical level, the width of cells corresponds to the road lane width. The polyline of the center of the road lane is provided by the HD map. We select a sampling step parameters to split this polyline in several parts. Each segment is then extrapolated on its both sides to build single cells. Through this sampling step parameter, we are able to refine more or less the level of detail of the

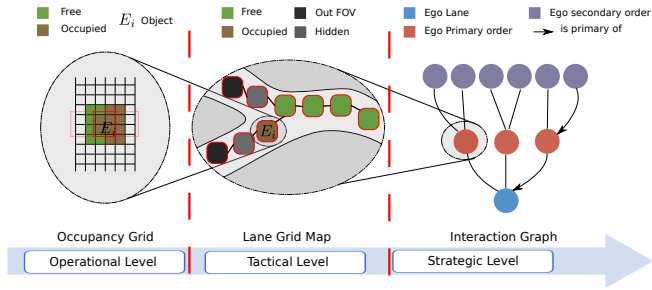


Fig. 2: Spatial information representation at each level of abstraction. The cells of the LGM are represented by the squared nodes.

information. Bigger are the cells, i.e. the less number of cells we have, the less information we have about the situation.

The LGM aims at augmenting the operational spatial representation (left part of figure 2) to provide non-misleading information. It gives information of spatial occupancy but also with a notion of along-track distances.

C. Characterization process

Within the true world, the cells of the LGM are either Free (F) or Occupied (O). However, in practice, some of the cells may be hidden because of occlusions and should be handled carefully. Therefore, in the characterization process of the cells of the LGM, the Hidden (H) class is considered explicitly along with F and O . Note that some cells are not observed not because they are hidden but because they are out of the field of view of the sensors. These cells will be ignored during the evaluation process.

The classification of the cells into one of the three aforementioned classes can be done via the use of probabilistic occupancy grids [16] or more robustly with evidential grids [17]. Another simpler way to achieve this characterization is using a free space polygon [9]. This type of approach has been implemented in this work.

D. Efficiency and scalability advantages

In classical occupancy grids (OG), all the space surrounding the vehicle is characterized regardless of their relevance. On the contrary, the LGM takes into account the situation in which the AV drives, i.e. in a given road layout, therefore it only stores information within the relevant lanes (AOI) provided by the Interaction Graph at the strategic level. As a consequence, the LGM encodes the information of the space surrounding the vehicle in a more compact and efficient way. Each cell of the LGM has two values: the width c_w , which corresponds to a lane level width and a sampling step length c_l . At the opposite, the OG is a spatial sampling over the entire space given square cells of width s_w . Let us consider an area of 50 m over 50 m ($A = 2500\text{m}^2$) that needs to be encoded in both representations with the same cells size.

The OG has a number of cells $C_{OG} = \frac{A}{s_w^2}$ and a visibility distance $d_{OG} = \sqrt{A}$ m as the OG covers a 50 m square. We assume that the vehicle is located in the center of both representations and let us take the example of a straight road lane. The LGM has a number of cells $C_{LGM} = \frac{A}{c_w \times c_l}$ and a

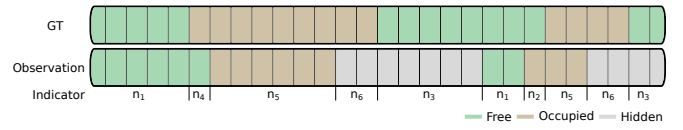


Fig. 3: Correspondence between evaluation parameters and the LGM of both the observation and the GT.

visibility distance $d_{LGM} = \frac{A}{c_w \times c_l} \times c_l = \frac{A}{c_w}$ m. For example:

$$\begin{aligned} c_w = 1\text{m} \\ c_l = s_w = 1\text{m} \end{aligned} \Rightarrow \begin{aligned} d_{LGM} = 50 \times d_{OG} \\ \text{with } C_{LGM} = C_{OG} \end{aligned} \quad (1)$$

The increase of the visibility distance is easily explained by the fact that cells are located in a focused area for the autonomous driving. Computationally we could raise the number of lanes by decreasing the visibility distance that would be dispatched on each lane.

It should be noticed that the LGM representation is easily scalable. Indeed, we can vary the sampling step and easily aggregate cells with low difficulty. On top of that, the fact that cells fit properly the road layout enables to have a good fidelity information representation over distances. Thus, this representation has the advantage to supply a coupled information. According to the situation encountered, it supplies occupancy information with distances.

In order to compare, if we look at OG used in the literature, these phenomena are two limitations. As cells are independent from the geometrical layer of the map, the delimitation of a number of cells to take into account for a portion of the road would not be easily defined. Distances over a grid are also not easy to fit as it does not reason in the coordinate system of the road lane.

IV. PERFORMANCE METRICS

This section presents the evaluation method used to demonstrate the effectiveness of the Lane Grid Map. This methodology introduces the integrity criterion. The metrics presented aim at providing two types of information in a single representation. At maneuver level for the DM, the LGM supplies both distances and occupancy for the task to be fulfilled.

A. Evaluation metrics

1) *Ground truth generation*: In order to validate the LGM model and efficiency, we want to compare the characterization process using the ground truth position of several vehicles. Given the precise position of several vehicles on the road and their dimensions, the occupancy of these vehicles are approximated as rectangles. All the cells overlapped by these rectangles are considered as occupied on the ground truth LGM. Then, the rest of the cells are considered as being free. The cells of the ground truth LGM are either Free (F) or Occupied (O). The top row in figure 3 shows the characterization of the LGM by the ground truth.

2) *Observation generation*: At the same time, we apply the characterization process with the on-board perception system. Using polygons approach, we have the two types of information: the convex bounding polygons of the perceived objects and a free-space polygon. The perception system is

TABLE I: Parameters obtained with the combination of the ground truth and the observation.

Ground Truth	Observation		
	f	o	h
F	$F : f \mapsto n_1$	$F : o \mapsto n_2$	$F : h \mapsto n_3$
O	$O : f \mapsto n_4$	$O : o \mapsto n_5$	$O : h \mapsto n_6$

described in section V. The bottom row in figure 3 shows the characterization by the ego vehicle of the cells of the LGM into one of the three states: F , O and H .

Over the ego vehicle trajectory, we record at each time step $t \in [0, T]$ the $LGM(t)$. At each time step we have the LGM characterized by the AV perception and also by the ground truth of the objects. Combining the different configurations, for each cell of the LGM, there are six possible indicators N_i obtained from the combination of both characterization as defined in table I. The correspondence is shown as an example on the indicator row of figure 3. As a cell depicts the occupancy of a fixed step distance, we can express these results not only in terms of cells but also in terms of distance and more precisely with a percentage. All the cells c^k of each LGM are associated with a distance $n_j^k \in \{n_1, \dots, n_6\}$. The indicators can be written as follows:

$$N_i = \sum_{t \in [0, T]} \sum_{c^k \in LGM(t)} \delta_{ij} * n_j^k \quad \text{with } \delta_{ij} = \begin{cases} 1 & \text{if } i = j \\ 0 & \text{if } i \neq j \end{cases} \quad (2)$$

Two indicators are particularly relevant for the integrity analysis. N_2 corresponds to miss-classified free cells considered as occupied. It is an overcautious indicator. N_4 is the most important indicator as it corresponds to the miss-classified occupied cells considered as free. It is a highly miss-leading indicator that should be as low as possible. Indeed, if we give information of free space around the vehicle whereas it is occupied it can leads to a hazardous decision-making. At the opposite, if occupied information is given instead of a free one, it remains a cautious situation for the DM. In section V we analyze the rates of these two indicators. The False Negative Rate (FNR) is the rate of N_4 over all occupied cells whereas the False Positive Rate (FPR) is the rate of N_2 over all free cells.

$$FNR = \frac{N_4}{N_4 + N_5 + N_6} \quad , \quad FPR = \frac{N_2}{N_1 + N_2 + N_3} \quad (3)$$

B. Integrity with localization and perception uncertainties

For autonomous navigation tasks, the spatial occupancy characterization must not provide misleading information. The goal is to provide information with a high level of confidence with the notion of integrity. For a given integrity risk level, the characterization error represented by the FNR must be below the set risk level. We will show that the main contribution brought by the LGM is its ability to keep the integrity of the information thanks to its capacity to control the FNR via the sampling step which has an impact on the overall LGM characterization performance.

In addition to that, we need to evaluate the integrity with the impact of the localization errors. As HD maps

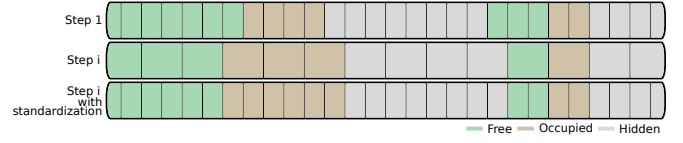


Fig. 4: Aggregation and standardization of the LGM from initial step to another.

are used to create the LGM in a global frame coordinates, perceived information in the AV local frame is transformed into the global frame thanks to the localization position. As a consequence, when the uncertainty of the localization is taken into account, the characterization process has to provide, whatever the situation is, a confidence level of the information stored. In order to evaluate the robustness of our model, we added some Gaussian noises with different standard deviations on the pose of our ground truth. Thus, we can study the impact of the localization uncertainty on our system.

At first, we consider that there is a noise on the localization but we do not model it in the perception outputs. We want to show that despite uncertainties, we are still able to manage the characterization process through the sampling step.

Usually localization estimation also quantifies its uncertainty, typically with a covariance matrix. This uncertainty can be propagated to the polygons by enlarging them. As localization errors on the AV position are introduced, the uncertainty is propagated on the object hulls when they are transformed from the local coordinates of the car to the world coordinates. We want to show that if we take a maximum allowed threshold of error for the misleading indicator, i.e. N_4 value, we are able to remain under this threshold thanks to the cells sampling step value. Thus, despite the uncertainty of the perception and the localization, we are able to guarantee a functional domain for the vehicle.

In order to vary the sampling step, we applied a methodology to replay the scenario for each step (figure 4). To proceed, we took the results for a minimum step (step 1 of figure 4), which is typically used for the ground truth, and combined them to increase the step. For instance, with a sampling step of 0.2 m we combined information of two cells of 0.1 m by applying an aggregation rule that gives an identical result as if we had run the process in real time (step i of figure 4). The aggregation rule is the same as in table II. Then, to be able to compare the ground truth with the initial step, the aggregated cells are split back to the standard minimal sampling step of the LGM used for the ground truth as shown in figure 4.

V. EXPERIMENTS

A. Setup

In order to validate our method, we analyze experiments carried out with three vehicles in real road conditions. The experiments were conducted with two experimental Renault ZOE vehicles and one Renault Master of the Heudiasyc laboratory. An HD map previously constructed in the city of Compiègne has been used to lead the experiments.

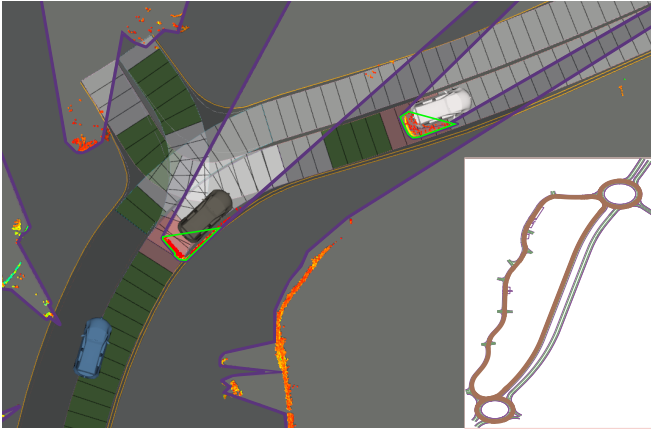


Fig. 5: Lane Grid Map displayed in RViz with three vehicles. The ego vehicle (blue) is following the two other ones (gray and white). Each cell is characterized as one of the following states: free (green), occupied (red), hidden (white). The free space polygon is shown in purple and objects polygons in green. The global path is displayed at the bottom right.

A NovAtel SPAN-CPT IMU with post-processed GNSS PPK corrections was used to have a centimeter-level accurate localization of each vehicle. A Velodyne VLP32-C LiDAR was used for the environment perception only in the ego vehicle. This sensor has a 360° field of view with a theoretical range of 100 meters and runs at 10 hz. It enables to build several types of spatial occupancy representation.

1) *Occupancy Grid (OG)*: With this representation, there are in the literature two methods to encode the space state: probabilistic grids [16] or evidential grids [8]. As illustrated in figure 2, the intersection between each cell of the LGM and the OG is computed such that one cell of the LGM encompasses N cells of the OG. When merging two cells information, the O state is more conservative than the H state which is more cautious than the F state. Therefore, we consider the following aggregation rule, table II, when characterizing cells of the LGM. The resulting cell is occupied if at least one cell is occupied and is free only if both cells are free. In other cases, the resulting cell is hidden.

2) *Polygons*: Instead of a grid, an approach based on polygons can be used. One can compare it for instance to a parametric free space [9]. The free space polygon F_p considers that the space inside is free (illustrated with a purple contour in figure 5). The occupancy of objects are given under a list of polygons O_p considered as being occupied. Thus, we can compute the intersection between each cell $Cell_i$ of the LGM and the different polygons. The results of these intersections provide the state $S(\cdot)$ of the cells:

$$\begin{aligned} & \text{if } (O_p \cap Cell_i) \neq \emptyset \text{ then } S(Cell_i) = O ; \\ & \text{else if } (F_p \cap Cell_i) = Cell_i \text{ then } S(Cell_i) = F ; \\ & \text{else } S(Cell_i) = H \end{aligned} \quad (4)$$

In our approach, the polygon method has been implemented for its practicality. A simple geometric ground fitting based on Principal Component Analysis algorithm and a clustering algorithm was used to measure the free space and

TABLE II: Aggregation rule of two OG cells. The information is condensed in the LGM cell.

		$Cell_{i+1}$		
		F	O	H
$Cell_i$	F	F	O	H
	O	O	O	O
	H	H	O	H

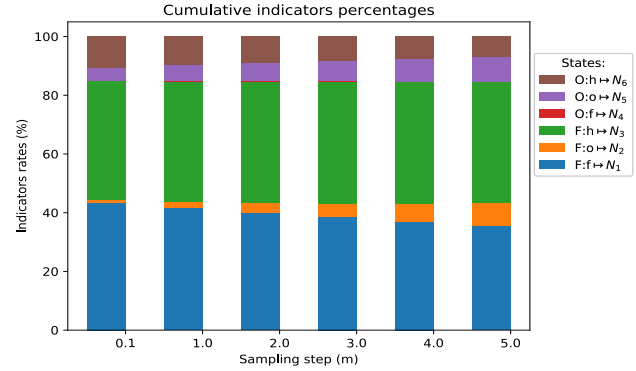


Fig. 6: Cumulative percentages of the six N_i indicators

object surrounding the ego vehicle [24]. A clustering has been used to extract objects clusters. Finally, the geometric layer of the HD map has been used to filter only objects on the road (figure 5).

The ego-vehicle and paths of interest are extracted recursively from the HD map as they can be pre-processed thanks to the topological layer. The *AOI* are represented by polygons using the center line with its width. The Robot Operating System (ROS) middle-ware was used for the implementation and the Boost Geometry library for the geometric operations between areas of interest and polygons.

A single dataset with sensors raw data has been recorded on an open road along a trajectory of 1.5 km in an urban area. The ego vehicle was following the two others all along the trajectory. That is why, during this scenario, only the clusters corresponding to the two perceived vehicles were used to compute the results.

When replaying data in real time, the LGM has been evaluated over 50 m in front of the ego vehicle as the two others were driving just in front of it (figure 5) and generated at a rate of 10hz. Firstly, the LGM has been recorded when replaying the dataset with a minimum sampling step of 0.1 m. In a second time, data were replayed in real time in order to simulate the same scenario but applying a Gaussian noise on the AV pose. It permits to add an error on the position with the same sensors and perception setup. We report six replays with standard deviation varying from 0 to 0.5 m. For each replay, there are two scenarios. The first one, without uncertainty propagation, the clusters size does not take into account the noise applied on the localization. The second one, with uncertainty propagation, a convex hull of each polygon object is augmented taking into account the localization uncertainty. We have used the method presented in [25]. Each vertex of the polygon of an object generates

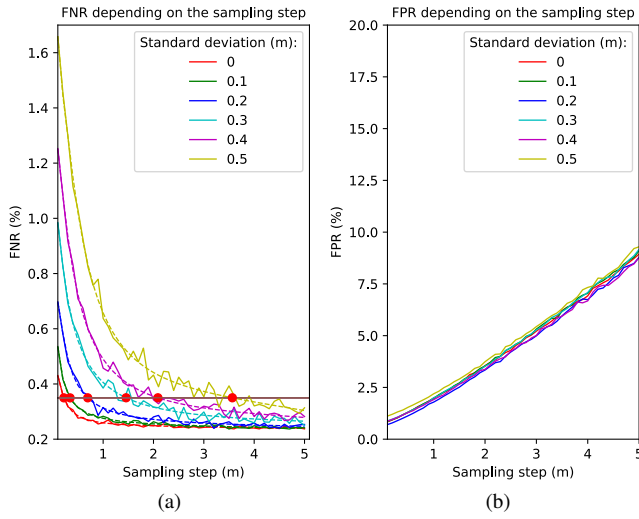


Fig. 7: FNR and FPR of the LGM without uncertainty propagation on the polygons of the detected vehicles. Random errors with different standard deviations are added to the localization estimates. The x-axis corresponds to the spatial sampling of the LGM.

several other vertices with a transformation that takes three times the standard deviation on the pose in each direction. Given all the resulting points, a new object convex hull is obtained and used in the characterization process.

In addition to that, given the fact that for each scenario we added simulations with a variation of the sampling step from 0.1 m to 5 m with a step of 0.1 m, it gives the equivalent of $6 \times 2 \times 50 = 600$ simulations to study the influence of the sampling step, the noise and the uncertainty propagation on the perception polygons.

Figure 6 depicts values that are computed at the end of one scenario, replayed in real time and for a sampling step $p_s \in [0.1, 5]$ m. It shows the cumulative sum of each indicator N_i for several sampling steps of the LGM cells.

B. Results

Figure 7 depicts results obtained by the replay of data without propagating the uncertainty on the polygons of the detected vehicles. On the left of the figure, the FNR of the misleading occupation is plotted in function of the sampling step of the LGM. On the right, the FPR of the over cautious occupation is also plotted in function of the sampling step. Each curve shows the evolution of the rate value depending on the standard deviation of the noise added on the pose.

Figure 7a shows a decreasing level of the FNR when the sampling step raises. Indeed, the cells classified as occupied get bigger and, therefore, they cover a larger space that encompasses nearby cells that were incorrectly classified as free because of the localization error. As the standard deviation of the noise increases, the FNR decreases but at a higher level. This shows that it is possible to decrease the FNR under a given integrity risk by increasing the sampling step. For example, if we set a maximum integrity risk of 0.35% for the FNR , the integrity requirement can be reached by setting the sampling step to the value depicted by the red dots in figure 7. To compute these red dots,

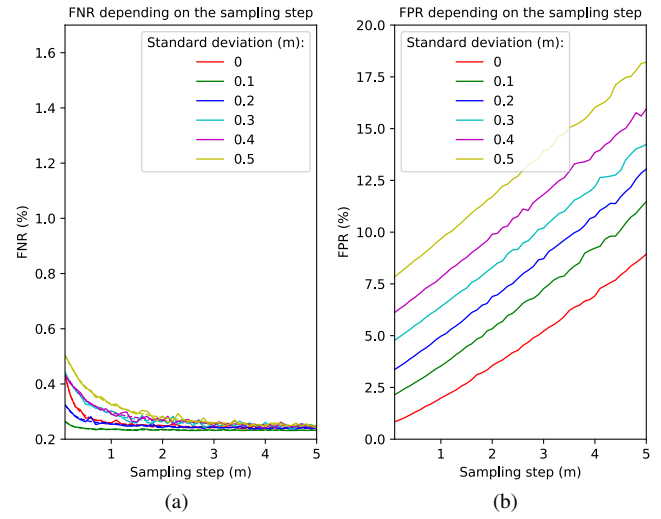


Fig. 8: FNR and FPR of the LGM with uncertainty propagation on objects hulls as described in section IV-B.

the different curves are interpolated in a logarithmic scale (dashed curves) and intersected with the required integrity risk. For a localization noise with a standard deviation of 0.5 m, we need a sampling step of around 3.5 m while for a standard deviation smaller than 0.2, a sampling step lower than 1 m is enough. The disadvantage of subsampling is that navigation quantities (such as distances to other vehicles, for example) may be too discrete to properly perform the current task. In other words, this graph shows that if we are not able to model the localization uncertainty, a correct sampling allows to keep the information safe as defined by the functional domain. For a given integrity risk, higher the uncertainty, higher the sampling step. The question can also be addressed the other way around: oversampling the LGM brings more misleading information since the curves increase as we get closer to zero.

On figure 7b, one can observe that the noise does not have influence on the FPR . As the aggregation rule is conservative on the occupied state, the FPR increases as the size of each occupied cell gets bigger. The superposition of each curve can be explained by the fact that, observing an occupied polygon, whatever the noise is, the size of the occupied polygon is not modified which does not change the impact on the cells.

Figure 8a shows the same curves as the previous figure with the difference that the uncertainty is now propagated onto the polygons which are enlarged. As a consequence, they cover a bigger space to ensure covering the correct occupied state. All the curves have the same shape with a much lower FNR . When the uncertainty is properly handled, we are therefore able to keep integrity at a given level for a shorter sampling step.

As it can be observed on figure 8b, the consequence of making the polygons bigger is a higher variation on the FPR depending on the standard deviation of the noise. It is explained by the fact that the perception system is much more conservative as occupied area gets bigger as localization uncertainty increases. When the noise model is estimated

and propagated, subsampling leads to a loss of efficiency as the FPR grows rapidly for no variation of the FNR . When uncertainty is taken into account and propagated to the polygons, it is possible to decrease the FNR while the FPR increases with the noise.

For a given integrity risk, with uncertainty propagation, it is therefore possible to lower the sampling step compared to no propagation. It brings us closer to a finer representation. If localization uncertainty is not well defined, in order to keep a target integrity at 0.35% for the FNR , the sampling step parameter should be equal or below 3.6 m. However, if uncertainty is well bounded, the sampling step parameter can be lowered to 1m. Thus, we are able to refine information stored by the LGM. As a consequence, if the localization uncertainty is well defined, a lower sampling step is suitable in order not to supply misleading information. A low integrity risk level can be chosen. However, if the estimation error is not well bounded, we need to use a higher sampling step to keep the same integrity risk level.

VI. CONCLUSION

In this paper, an intermediate lane level information representation has been deepened with Lane Grid Maps. This representation aims at providing spatial information at a lane level to the maneuver planner of a decision-making module. We have demonstrated the capability of such a representation to help providing non-misleading information given an integrity risk. A LGM provides a spatial information representation in the road lane frame. This grid is sampled and each cell supplies spatial state information among: free, occupied or hidden. Based on its sampling step parameters, a confidence value of the information has been evaluated and compared to the ground truth of vehicles with real experiments. We demonstrated the need to find a proper sampling step for keeping information integrity under a given target. Indeed, oversampling can lead to increase misleading information, in addition to requesting heavier calculations to be done in real time. A proper sampling step is thus necessary depending on uncertainty management. The methodology we have presented in this article allows to answer this question.

In future work, situation predictions based on this representation will also be explored.

REFERENCES

- [1] S. Ulbrich, A. Reschka, J. Rieken, S. Ernst, G. Bagschik, F. Dierkes, M. Nolte, and M. Maurer, "Towards a Functional System Architecture for Automated Vehicles," *arXiv:1703.08557*, Mar. 2017.
- [2] F. von Hundelshausen, M. Himmelsbach, F. Hecker, A. Mueller, and H. J. Wuensche, "Driving with tentacles: Integral structures for sensing and motion," *Journal of Field Robotics*, vol. 25, pp. 640–673, 2008.
- [3] P. F. Orzechowski, C. Burger, and M. Lauer, "Decision-making for automated vehicles using a hierarchical behavior-based arbitration scheme," in *IEEE Intelligent Vehicles Symposium*, 2020, pp. 767–774.
- [4] M. Althoff, O. Stursberg, and M. Buss, "Model-Based Probabilistic Collision Detection in Autonomous Driving," *IEEE Transactions on Intelligent Transportation Systems*, vol. 10, pp. 299–310, Jun. 2009.
- [5] Z. Papp, C. Brown, and C. Bartels, "World modeling for cooperative intelligent vehicles," in *IEEE Intelligent Vehicles Symposium*, Jun. 2008, pp. 1050–1055.
- [6] L. Sun, W. Zhan, C.-Y. Chan, and M. Tomizuka, "Behavior Planning of Autonomous Cars with Social Perception," in *IEEE Intelligent Vehicles Symposium*, Jun. 2019, pp. 207–213.
- [7] P. Schorner, L. Tottel, J. Doll, and J. M. Zollner, "Predictive Trajectory Planning in Situations with Hidden Road Users Using Partially Observable Markov Decision Processes," in *IEEE Intelligent Vehicles Symposium*, Jun. 2019, pp. 2299–2306.
- [8] H. Mouhaghir, V. Cherfaoui, R. Talj, F. Aioun, and F. Guillemand, "Using evidential occupancy grid for vehicle trajectory planning under uncertainty with tentacles," in *2017 IEEE 20th International Conference on Intelligent Transportation Systems*, Oct. 2017, pp. 1–7.
- [9] M. Schreier, V. Willert, and J. Adamy, "Compact Representation of Dynamic Driving Environments for ADAS by Parametric Free Space and Dynamic Object Maps," *IEEE Transactions on Intelligent Transportation Systems*, vol. 17, no. 2, pp. 367–384, Feb. 2016.
- [10] S. Ulbrich, T. Menzel, A. Reschka, F. Schuldt, and M. Maurer, "Defining and Substantiating the Terms Scene, Situation, and Scenario for Automated Driving," in *IEEE 18th International Conference on Intelligent Transportation Systems*, Sep. 2015, pp. 982–988.
- [11] J. A. Hage, P. Xu, P. Bonnifait, and J. Ibanez-Guzman, "Localization Integrity for Intelligent Vehicles Through Fault Detection and Position Error Characterization," *IEEE Transactions on Intelligent Transportation Systems*, pp. 1–13, 2020.
- [12] C. Sanchez, P. Xu, A. Armand, and P. Bonnifait, "Lane level context and hidden space characterization for autonomous driving," in *IEEE Intelligent Vehicles Symposium*, 2020, pp. 144–149.
- [13] J. A. Michon, "A Critical View of Driver Behavior Models: What Do We Know, What Should We Do?" in *Human Behavior and Traffic Safety*. Springer US, 1985, pp. 485–524.
- [14] C. Lundquist and T. B. Schön, "Estimation of the Free Space in Front of a Moving Vehicle," in *SAE World Congress & Exhibition*, Apr. 2009, pp. 2009-01-1288.
- [15] F. Poggenhans, J.-H. Pauls, J. Janosovits, S. Orf, M. Naumann, F. Kuhnt, and M. Mayr, "Lanelet2: A high-definition map framework for the future of automated driving," in *IEEE International Conference on Intelligent Transportation Systems*, Nov. 2018, pp. 1672–1679.
- [16] C. Chen, C. Tay, C. Laugier, and K. Mekhnacha, "Dynamic Environment Modeling with Gridmap: A Multiple-Object Tracking Application," in *IEEE International Conference on Control, Automation, Robotics and Vision*, Dec. 2006, pp. 1–6.
- [17] J. Moras, V. Cherfaoui, and P. Bonnifait, "Credibilist occupancy grids for vehicle perception in dynamic environments," in *IEEE International Conference on Robotics and Automation*, 2011, pp. 84–89.
- [18] T. Weiherer, S. Bouzouraa, and U. Hofmann, "An interval based representation of occupancy information for driver assistance systems," in *IEEE International Conference on Intelligent Transportation Systems*, Oct. 2013, pp. 21–27.
- [19] R. Danescu and S. Nedevschi, "A Particle-Based Solution for Modeling and Tracking Dynamic Digital Elevation Maps," *IEEE Transactions on Intelligent Transportation Systems*, vol. 15, pp. 1002–1015, Jun. 2014.
- [20] M. M. Minderhoud and P. H. Bovy, "Extended time-to-collision measures for road traffic safety assessment," *Accident Analysis & Prevention*, vol. 33, no. 1, pp. 89–97, Jan. 2001.
- [21] S. Noh, "Decision-Making Framework for Autonomous Driving at Road Intersections: Safeguarding Against Collision, Overly Conservative Behavior, and Violation Vehicles," *IEEE Transactions on Industrial Electronics*, vol. 66, no. 4, pp. 3275–3286, Apr. 2019.
- [22] S. Shalev-Shwartz, S. Shammah, and A. Shashua, "On a Formal Model of Safe and Scalable Self-driving Cars," *arXiv:1708.06374*, Aug. 2017.
- [23] N. Zhu, J. Marais, D. Betaille, and M. Berbineau, "GNSS Position Integrity in Urban Environments: A Review of Literature," *IEEE Transactions on Intelligent Transportation Systems*, vol. 19, no. 9, pp. 2762–2778, Sep. 2018.
- [24] D. Zermas, I. Izzat, and N. Papanikolopoulos, "Fast segmentation of 3D point clouds: A paradigm on LiDAR data for autonomous vehicle applications," in *IEEE International Conference on Robotics and Automation*, May 2017, pp. 5067–5073.
- [25] E. Bernardi, S. Masi, P. Xu, and P. Bonnifait, "High Integrity Lane-level Occupancy Estimation of Road Obstacles Through LiDAR and HD Map Data Fusion," in *IEEE Intelligent Vehicles Symposium*, Oct. 2020, pp. 1873–1878.